Scientific Papers. Series E. Land Reclamation, Earth Observation & Surveying, Environmental Engineering. Vol. XV, 2026
Print ISSN 2285-6064, CD-ROM ISSN 2285-6072, Online ISSN 2393-5138, ISSN-L 2285-6064

SEISMIC RESPONSE ANALYSIS OF A LONG-TERM MONITORED BUILDING USING CO-LOCATED STRUCTURAL AND FREE-FIELD RECORDS

Iolanda-Gabriela CRAIFALEANU[1, 3], Claudiu-Sorin DRAGOMIR[1, 2], Daniela DOBRE[1, 3], Emil Sever GEORGESCU[1], Alexandra-Marina BARBU[1]

[1]National Institute for Research and Development in Constructions, Urbanism and Sustainable Spatial Development, URBAN-INCERC, 266 Pantelimon Road, District 2, Bucharest, Romania
[2]University of Agronomic Sciences and Veterinary Medicine of Bucharest, 59 Mărăști Blvd, District 1, Bucharest, Romania
[3]Technical University of Civil Engineering Bucharest, 122-124 Lacul Tei Blvd, District 2, 020396, Bucharest, Romania

Corresponding author email: iolanda@incd.ro

Abstract

Monitoring building vibrations provides important information on structural health and, through on the detection of changes in dynamic characteristics, can serve as an early indicator of potential degradation or damage. However, detection reliability depends substantially on appropriate instrumentation capable of clearly capturing the building response to ambient, natural and anthropogenic vibrations. The paper presents an in-depth study based on data recorded during recent seismic events on a higher-education building in Bucharest, Romania. The building has been continuously monitored for vibrations for more than a decade. Unlike many other urban buildings monitored in Romania, the building's location within a university campus - characterized by large open spaces - enabled the installation of a free-field-type station approximately 30 m away from the building, such that reference ground motion records were also available. Based on multiple types of analyses, the study provides valuable insights into the building's dynamic characteristics, soil-structure interaction phenomena and kinematic effects.

Key words*: building vibrations, dynamic characteristics, kinematic effects, soil–structure interaction, structural health monitoring.*

INTRODUCTION

Monitoring building vibrations is an essential tool for the rapid detection of potentially unsafe changes in structural dynamic characteristics, which may indicate degradation or damage. However, especially in urban environments, complete instrumentation is often challenging, due to the difficulty of identifying open spaces for installing reference free-field stations in the vicinity of the building (COSMOS, 2001; Skolnik, 2010). The National Institute for Research and Development in Constructions, Urbanism and Sustainable Spatial Development, URBAN-INCERC (NIRD URBAN-INCERC) has a long history of activities in the field, with the first seismic stations installed on buildings in the late 1960s and early 1970s (Berg et al., 1977; Bălan et al., 1982). A large campaign of temporary building instrumentation was carried out in the years preceding the catastrophic March 4, 1977, M = 7.2 earthquake. The dynamic characteristics (natural periods of vibration) measured within this campaign on 47 buildings in Bucharest (Bălan et al., 1982) provided essential information for assessing their post-earthquake condition. In the years that followed, several buildings in Bucharest and in other major cities were permanently instrumented. After 1990, despite the reduction of the number of instrumented buildings (mainly due to ownership changes and equipment obsolescence), both temporary and permanent instrumentation for building vibrations monitoring continued. A large-scale, multi-annual campaign - still ongoing within the "Nucleu" Programme PN 23 35 "ECODIGICONS" - has focused on the temporary instrumentation of several public buildings and the determination of their reference dynamic characteristics, particularly

for those hosting national research and development institutes. The campaign is carried on through the National Network for the Seismic Monitoring and Protection of the Building Stock (RNMPSPC), an infrastructure of national interest operating within NIRD URBAN-INCERC (https://incd.ro/reteaua-nationala-de-monitorizare-siprotectie-seismica-a-patrimoniului-construit-iosin/).

The building examined in this study has been subjected to continuous vibration monitoring for over a decade. Unlike many other urban buildings monitored in Romania, the building's location within a university campus – characterized by large open spaces – enabled the installation of a free-field-type station approximately 30 m away from the building, such that reference ground motion records are also available. Based on multiple types of analyses, this study aims to provide valuable insights into the building's dynamic characteristics, soil-structure interaction phenomena, and kinematic effects.

MATERIALS AND METHODS

Description of the monitored building

The monitored building is situated on the campus of the University of Agriculture and Veterinary Medicine in Bucharest and serves as the headquarters of the Faculty of Biotechnologies (Figures 1 and 2). The campus, with a surface area of 38 hectares, benefits from large spaces between the buildings, arranged as parks and recreational areas.

The building, completed in 2016, comprises a basement and three above-ground stories. Its structural system consists of reinforced concrete frames combined with shear walls.

The instrumentation system, installed ever since the building completion, consists of a Kinemetrics Granite digitizer and recorder, with ES-T triaxial episensors placed in the basement, at the roof of the building and in a special encasement, located about 30 m away from the building, in a neighbouring green space (Figure 3). The digitizer, placed in the central building section, is equipped with 12 channels, of which channels 1-3, 5-7 and 9-11 are assigned, in order, to vibration measurements at the three mentioned locations: free field, basement and roof. Channels are identified as HNZ, HNN and HNE, respectively, with suffixes indicating the location (FF – free field, B1 – basement, 04 – roof).



Figure 1. Monitored building: Faculty of Building Technologies of the University of Agronomic Sciences and Veterinary Medicine of Bucharest

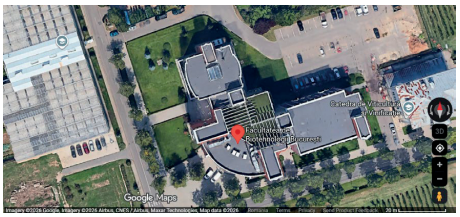


Figure 2. Map location and orientation of the monitored building (Google Maps screenshot) (https://www.google.com/maps/place/Facultatea+de+Biotehnologii+Bucure%C8%99ti/@44.4699931,26.0620898,132m/data=!3m1!1e3!4m6!3m5!1s0x40b2023b3338d51f:0xa7a705d357d7ce12!8m2!3d44.4696946!4d26.0625279!16s%2Fg%2F1hc0sxqyv?entry=ttu&g_ep=EgoyMDI2MDQwMS4wIKXMDSoASAFQAw%3D%3D)



a) b) c)

Figure 3. Station BTH: a) free-field station encasement, b) free-field episensor, c) installation of permanent online connection with the Data Centre of NIRD URBAN-INCERC

The station, identified by the code BTH, is permanently connected to the Data Centre of NIRD URBAN-INCERC, enabling the continuous acquisition of co-located structural and free-field seismic records. Through a secure communication link provided by the

Romanian Special Telecommunications Service, STS, the station transmits real-time data to the SeisComP (https://www.gempa.de/products/seiscomp/) seismological software running on the main server of the centre.

Ground motions considered

Ground motions recorded from two significant earthquakes (M_L = 5.2 and M_L = 4.8) originating in the Vrancea seismic zone of Romania, with epicentres located approximately 200 km from the building site, were used in the study. Their main characteristics, according to the website of the National Institute for Earth Physics (https://www.infp.ro/), are shown in Table 1.

Processing and analyses

The processing steps and analyses performed are presented below, with explanations on their meaning and relevance for the current study. The processing was carried out using the ViewWave software (Kashima, 2016; 2024).

Acceleration, velocity, and displacement waveforms

The recorded waveforms illustrate the temporal variation of the vibrations measured by sensors placed at different locations in the structure and in its vicinity. They also show the peak values reached during the earthquake, the amplification between the base and the roof of the building, as well as the primary differences between the free field motion and the motion recorded in the building's basement, at the foundation level.

Table 1. Main characteristics of Vrancea earthquakes considered in the study

Date and time (UTC)	Focal depth (km)	Epicentral coordinates	Local magnitude (M_L)
31.01.2020, 01:37:52	118.2	45.6937°N 26.6918°E	5.2
03.12.2023, 22:05:48	133.3	45.5939°N 26.4734°E	4.8

Husid plots

Husid plots illustrate the evolution of normalized Arias intensity throughout the seismic motion. They can be also used to estimate the significant duration of the earthquake (the duration of strong ground shaking), which is important for assessing its destructive potential by indicating when the largest amount of energy is induced during the event. Arias intensity is defined by the following equation:

$$I_A = \frac{\pi}{2g} \int_0^{T_d} a^2\,(t)\,dt \qquad (1)$$

where T_d is the duration of the ground motion and $a(t)$ is the acceleration.

Fourier and power spectra

Fourier analysis is the most widely used method for estimating the dynamic characteristics of a structure. This analysis transforms measured structural vibrations from the time domain to the frequency domain, allowing the identification of the natural frequencies of the structure, which generally correspond to the peaks of the Fourier amplitude spectra. Estimating the values of these natural frequencies provides a reference point for identifying future degradation or damage that alters the dynamic parameters of the structure, thus enabling structural health monitoring.

The *power spectrum* highlights the predominant frequencies/periods of the ground or structure vibration, the distribution of earthquake-induced energy over frequency ranges, and the bandwidth characteristic of the motion.

Response spectra

The following spectra and diagrams were determined:

- the acceleration spectrum (*Sa*);
- the velocity spectrum (*Sv*);
- the displacement spectrum (*Sd*);
- the pseudovelocity spectrum (*pSv*);
- the input energy spectrum (equivalent velocity) (*Ve*).

The *acceleration, velocity, and displacement spectra* are standard seismic record processing tools used to highlight the frequency content of ground motion, amplification effects, and related phenomena.

The *pseudovelocity spectrum* is computed by multiplying the ordinates of the relative displacement spectrum (Sd) by the corresponding circular frequency (ω):

$$pSv = \omega \cdot Sd \qquad (2)$$

The pseudovelocity spectrum is proportional to the elastic deformation energy of the system and serves as an indicator of the frequencies/periods associated with the maximum destructive potential of seismic motion, with direct applications in structural engineering.

Another important indicator is the *total input energy induced by the earthquake* (E). This is often expressed through the equivalent velocity V_E, defined by:

$$V_E = \sqrt{\frac{2E}{m}} = \sqrt{-2\int_0^{T_d} \ddot{x}_g(t)\dot{x}(t)dt} \quad (3)$$

where m is the mass, $\ddot{x}_g(t)$ and $\dot{x}_g(t)$ are the ground acceleration and relative velocity of the oscillator, respectively, and t is the time. The equivalent velocity (and thus the energy, E) is a significant measure of the destructive potential of seismic motion, with various structural engineering applications as well. It has the advantage of representing a scalar value, rather than a vectorial value.

Spectral ratios – transfer functions

The analysis of the *ratios* between the *Fourier amplitude spectra* recorded at the roof and those recorded at the base/foundation is another widely used method for determining the natural frequencies/periods of the structure, revealing the transfer functions. These ratios exhibit pronounced peaks at those frequencies. Such analyses are especially important for Structural Health Monitoring (SHM), because performing them at different time intervals allows detection of changes in the structure's dynamic characteristics. When free-field records are available near the building, comparing the Fourier amplitude spectra of the motions recorded at the foundation with those in free-field reveals the modification of free-field motion by the buildings' presence and the influence of soil–structure interaction.

RESULTS AND DISCUSSIONS

The obtained results are presented selectively in the following, with focus on the most significant observations and on the larger-magnitude earthquake.

Figure 4 presents the acceleration waveforms recorded during the 31 January 2020 earthquake. The P- and S-wave arrivals, as well as the amplitude and timing differences can be noticed. For each recording channel, the maximum acceleration amplitudes (a_{max}) are marked on the plot and summarized in Table 2, together with the corresponding maximum velocities (v_{max}), displacements (d_{max}), and Arias intensities (I_A). The table also includes the values recorded during the second earthquake considered, i.e., the one on 3 December 2023.

Figure 5 displays the Husid plots for the 31 January 2020 earthquake. As it can be noticed, the onset of the most pronounced intensity increase occurs around second 50 of the record, indicating when the maximum amount of energy is induced during this event.

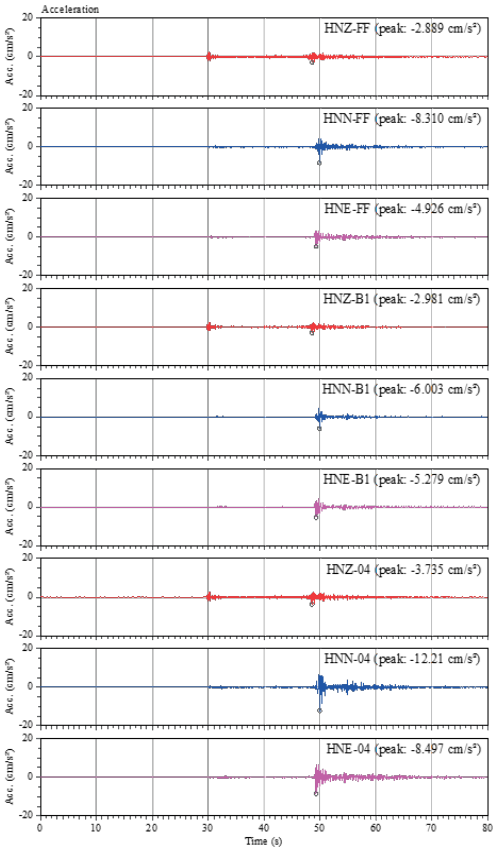


Figure 4. Acceleration waveforms for the 31.01.2020 earthquake

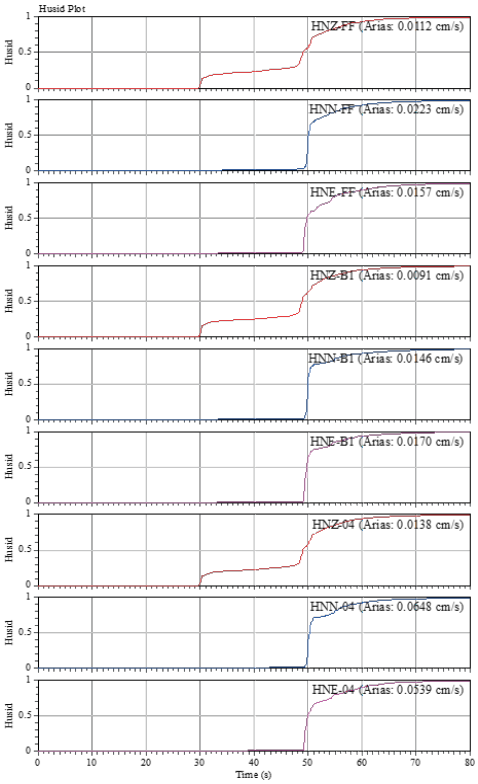


Figure 5. Husid plots for the 31.01.2020 earthquake

Values in Table 2 also show that, as expected, all ground motion parameters recorded for the 3 December 2023 (M_L=4.8) event are below those of the 31 January 2020 (M_L=5.2) event. They also reflect the differences in the spectral content of the two earthquakes considered.

In what concerns the variation of the parameters between the FF (free field), B1 (basement) and 04 (roof) sensors, an interesting attenuation of the amplitudes of the ground motion by the building, on certain frequency ranges, can be noticed – from FF to B1 – for the HNN components and, as a weaker effect, for the HNZ components. Regarding the B1–04 variation, amplification is observed consistently, on wide frequency ranges, especially for the horizontal channels. The features are also noticeable in Figure 6. These general amplification patterns are observable for both earthquakes.

An analysis of the spectral content of the FF, B1 and 04 components, as reflected by the acceleration spectra in Figure 6 and the values in Table 3, shows that the largest spectral peaks occur at short periods ($T < 0.5$ s) for both earthquakes, with differences regarding the dominant peaks of the spectra, but with similarities in the location of other peaks, which are persistent for both earthquakes.

Table 2. Maximum values of accelerations (a_{max}), velocities (v_{max}), displacements (d_{max}), and Arias intensities (I_A) for the earthquakes of 31 January 2020 (M_L = 5.2) and 3 December 2023 (M_L =4.8)

	31.01.2020 Earthquake (M_L = 5.2)				03.12.2023 Earthquake (M_L = 4.8)			
Channel	a_{max} (cm/s^2)	v_{max} (cm/s)	d_{max} (cm)	I_A (cm/s)	a_{max} (cm/s^2)	v_{max} (cm/s)	d_{max} (cm)	I_A (cm/s)
HNN-04	12.210	0.522	0.0456	0.0648	4.049	0.155	0.0083	0.0053
HNE-04	8.497	0.428	0.0388	0.0539	2.015	0.094	0.0076	0.0031
HNZ-04	3.735	0.124	0.0094	0.0138	2.254	0.042	0.0020	0.0019
HNN-B1	6.003	0.344	0.0332	0.0146	1.669	0.066	0.0044	0.0011
HNE-B1	5.279	0.277	0.0314	0.0170	1.089	0.074	0.0068	0.0009
HNZ-B1	2.981	0.121	0.0093	0.0091	1.912	0.039	0.0020	0.0013
HNN-FF	8.310	0.366	0.0353	0.0223	2.459	0.083	0.0046	0.0018
HNE-FF	4.926	0.278	0.0320	0.0157	1.121	0.072	0.0069	0.0010
HNZ-FF	2.889	0.119	0.0089	0.0112	2.068	0.040	0.0030	0.0015

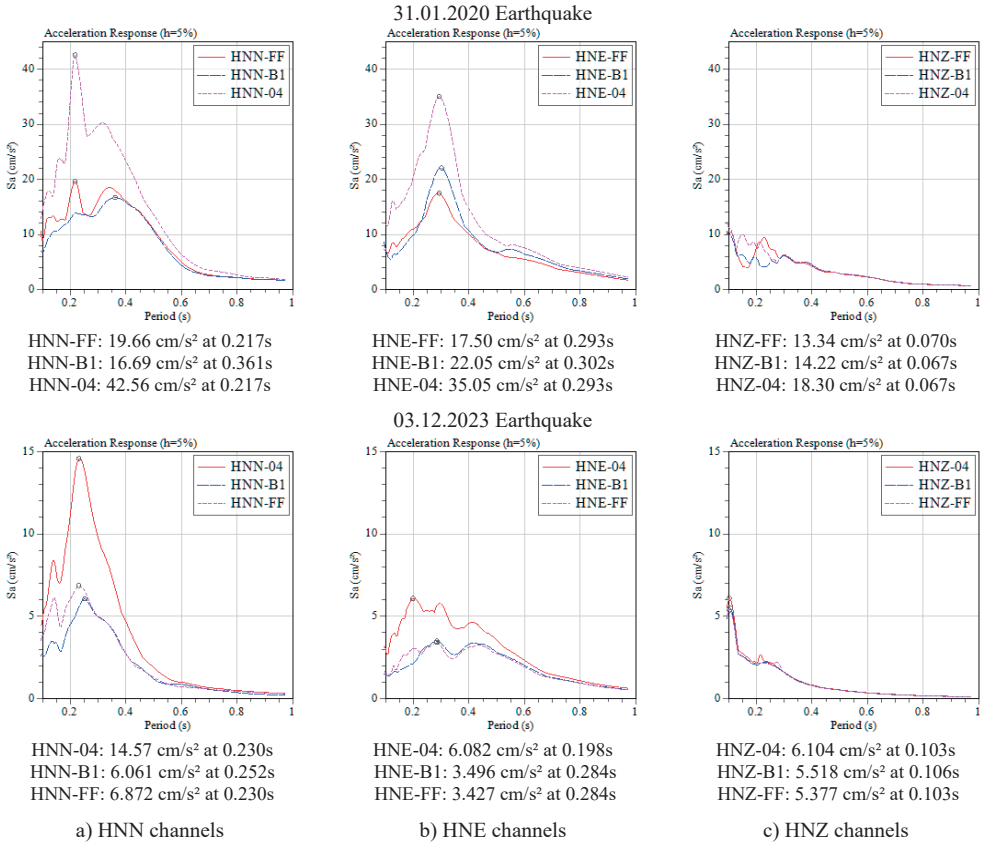


Figure 6. Acceleration spectra (5% damping) for the 31.01.2020 and 03.12.2023 earthquakes

Table 3. Periods corresponding to the maximum peaks if the acceleration spectra for the earthquakes of 31 January 2020 ($M_L = 5.2$) and 3 December 2023 ($M_L = 4.8$)

Channel	31.01.2020 Earthquake ($M_L = 5.2$)	03.12.2023 Earthquake ($M_L = 4.8$)
HNN-04	0.217s	0.230s
HNE-04	0.293s	0.198s
HNZ-04	0.067s	0.103s
HNN-B1	0.361s	0.252s
HNE-B1	0.302s	0.284s
HNZ-B1	0.067s	0.106s
HNN-FF	0.217s	0.230s
HNE-FF	0.293s	0.284s
HNZ-FF	0.070s	0.103s

Power spectra (with values listed in Table 4 and illustrated in Figure 7) show a more differentiated situation, given their multiple peaks, characteristic to a broadband motion. For the 31.01.2020 earthquake, a persisting period of approximately 0.44 seconds can be noticed on the HNN channels, where amplitudes increase progressively from FF to B1 and then, to 04.

Table 4. Periods corresponding to the dominant peaks of the power spectra, 30.01.2020 and 3.12.2023 earthquakes

Channel	30.01.2020	03.12.2023
HNN-04	0.235	0.225
HNE-04	0.306	0.181
HNZ-04	0.183	0.254
HNN-B1	0.439	0.314
HNE-B1	0.328	0.311
HNZ-B1	0.352	0.113
HNN-FF	0.442	0.314
HNE-FF	0.330	0.288
HNZ-FF	0.235	0.113

For the HNN-04 channel (roof), the 0.44 seconds peak is not the dominant one, as it is exceeded by the peak at $T = 0.235$ s, which most probably indicates the fundamental period

of vibration of the building on this direction, including the effects of soil-structure interaction (SSI). For the HNE channels, the FF and B1 records exhibit a clear peak at $T \approx 0.33$ s, visible also for the 04 records. The dominant peak for the roof record HNE-04 is slightly shifted to a shorter period, $T = 0.306$ s, which probably identifies the fundamental period of vibration of the building, including SSI effects, for this direction. The vertical (HNZ) channels exhibit the highest peaks at 0.235 s (FF), 0.352 s (B1) and 0.183 s (04). Again, the value $T = 0.183$ s could indicate the natural period of the structure on this direction, including SSI effects.

These assumptions will be however checked in the next section, where the transfer functions will be analysed as well.

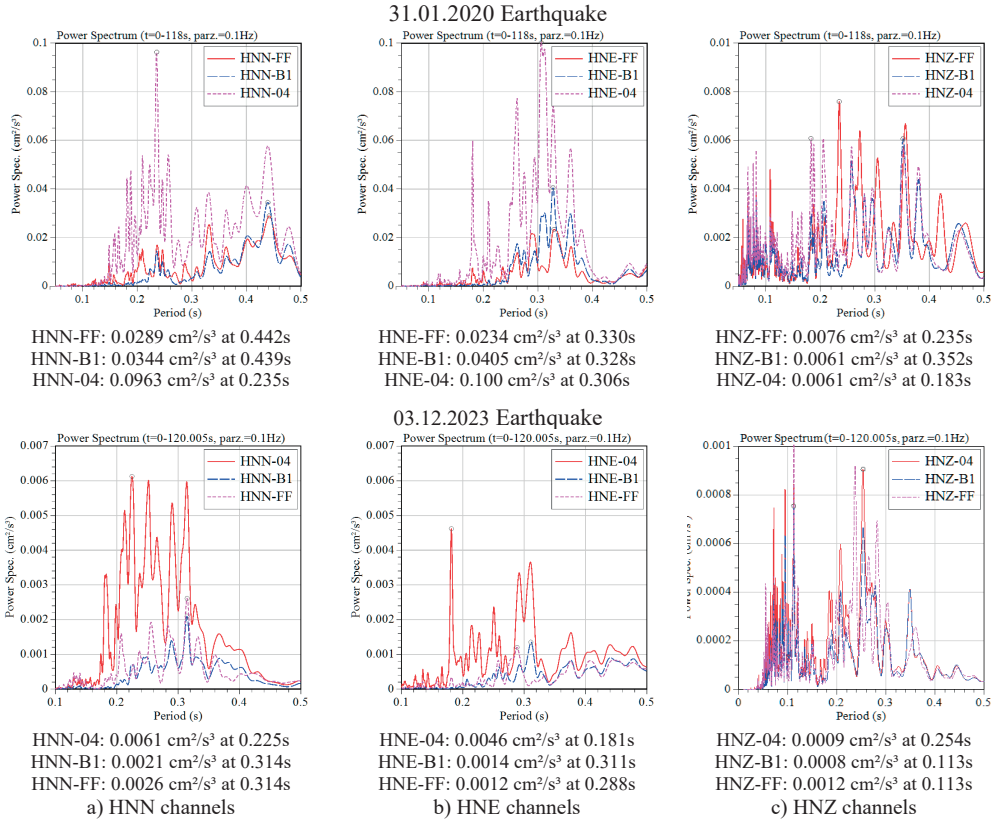


Figure 7. Power spectra for the 31.01.2020 and 03.12.2023 earthquakes

For the 03.12.2023 earthquake, the power spectra exhibit different patterns, as compared to the 31.01.2020 event. However, the two earthquakes share some common or close peaks.

Table 5 synthesizes the maximum Fourier amplitudes and their corresponding periods for the two earthquakes considered. The table shows marked differences between the two seismic events, especially the variation of amplitudes.

The pseudovelocity spectra and the equivalent velocity spectra (normalized input energy) are displayed in Figures 8 and 9, for the seismic event of 31.01.2020, while the periods corresponding to their dominant spectral peaks are synthesized in Table 6.

The spectral shapes are overall quite similar, even though their highest spectral peaks occur at different periods. The most noticeable difference appears in the spectral shapes associated with the HNN-04 channel, but also for HNZ-04.

Table 5. Maximum Fourier amplitudes and corresponding periods for the two earthquakes considered

Channel	31.01.2020 Earthquake		03.12.2023 Earthquake	
	Fourier max. amplitude (cm/s)	T (s)	Fourier max. amplitude (cm/s)	T (s)
HNN-04	3.973	0.235	0.654	0.314
HNE-04	4.047	0.306	0.444	0.288
HNZ-04	0.998	0.183	0.445	0.113
HNN-B1	2.375	0.439	0.587	0.314
HNE-B1	2.577	0.328	0. 471	0.311
HNZ-B1	0.997	0.352	0.352	0.113
HNN-FF	2.175	0.442	1.002	0.225
HNE-FF	1.958	0.330	0.870	0.181
HNZ-FF	1.116	0.235	0.385	0.254

Table 6. Periods corresponding to the highest spectral peaks of the pseudovelocity spectra and of the equivalent velocity spectra (normalized input energy), 31.01.2020 earthquake

Channel	From pseudovelocity spectra	From normalized input energy spectra
HNN-04	0.340	0.237
HNE-04	0.302	0.311
HNZ-04	0.383	0.204
HNN-B1	0.432	0.432
HNE-B1	0.311	0.330
HNZ-B1	0.383	0.361
HNN-FF	0.372	0.432
HNE-FF	0.302	0.330
HNZ-FF	0.230	0.276

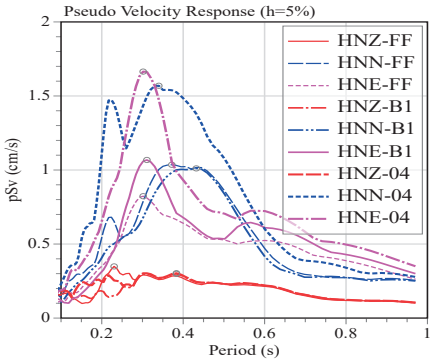


Figure 8. Pseudovelocity spectra for the 31.01.2020 earthquake

However, for HNN-04, both spectra have a peak at $T = 0.22$ - 0.237 s, which is consistent with the values obtained from the power spectrum and which also indicates a maximum of the energy induced by the earthquake.

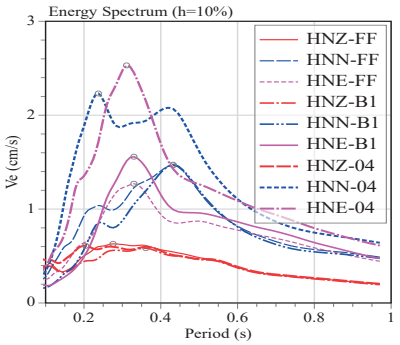


Figure 9. Equivalent velocity spectra (normalized input energy) for the 31.01.2020 earthquake

A distinct part of the study focused on transfer functions, both from the basement to the roof of the building and between the free-field motion and the basement motion. The first type of transfer function provides insight into the natural periods of the building, while the second type highlights how the presence of the structure modifies the motion of the surrounding soil.

Figures 10 and 11 show the transfer functions from basement to roof, while Figures 12 and 13 show the transfer functions from free field to basement motion.

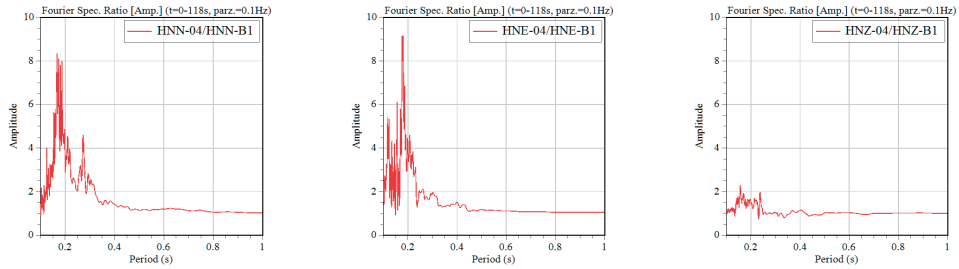
Tables 7 and 8 show the periods corresponding to the dominant peaks of the transfer functions between the foundation motion and the roof motion and, respectively, between the ground motion and the foundation motion. The first set of values is generally used to represent the natural vibration periods of the building, while the second set serves for highlighting the influence of the buildings' presence.

Table 7. Periods corresponding to the highest peaks of the transfer functions between the foundation and the roof motions - 31.01.2020 and 03.12.2023

Channels	31.01.2020	03.12.2023
HNN-04/HNN-B1	0.167 s	0.179 s
HNE-04/HNE-B1	0.180 s	0.179 s
HNZ-04/HNZ-B1	0.157 s	0.180 s

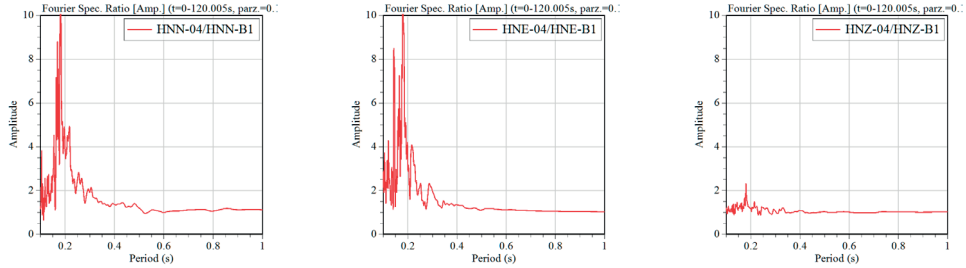
Table 8. Periods corresponding to the highest peaks of the transfer functions between the ground motion and the foundation motion - 31.01.2020 and 03.12.2023

Channels	31.01.2020	03.12.2023
HNN-B1/HNN-FF	0.256 s	0.272 s
HNE- B1/HNE-FF	0.314 s	0.309 s
HNZ- B1/HNZ-FF	0.256 s	0.256 s



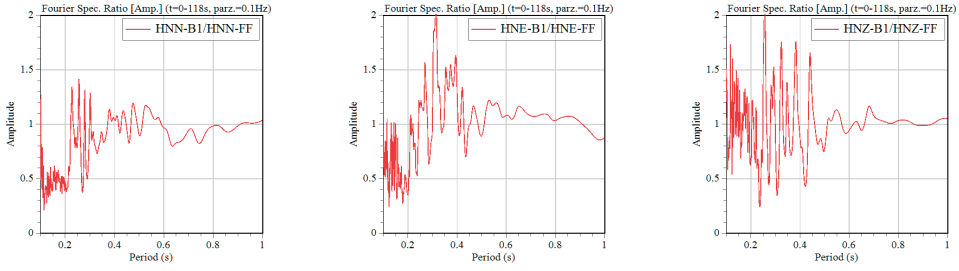
a) HNN-04/HNN-B1: 8.329 at 0.167 s b) HNE-04/HNE-B1: 9.145 at 0.180 s c) HNZ-04/HNZ-B1: 2.278 at 0.157 s

Figure 10. Transfer functions (basement – roof), 31.01.2020 earthquake



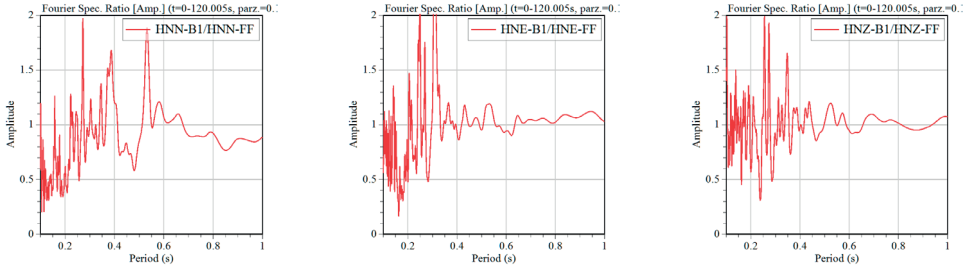
a) HNN-04/HNN-B1: 10.76 at 0.179 s b) HNE-04/HNE-B1: 12.88 at 0.179 s c) HNZ-04/HNZ-B1: 2.307 at 0.180 s

Figure 11. Transfer functions (basement – roof), 03.12.2023 earthquake



a) HNN-B1/HNN-FF: 1.413 at 0.256 s b) HNE-B1/HNE-FF: 2.058 at 0.314 s c) HNZ-B1/HNZ-FF: 2.228 at 0.256 s

Figure 12. Transfer functions (ground – foundation), 31.01.2020 earthquake



a) HNN-B1/HNN-FF: 1.973 at 0.272 s b) HNE-B1/HNE-FF: 3.417 at 0.309 s c) HNZ-B1/HNZ-FF: 1.870 at 0.256 s

Figure 13. Transfer functions (ground - foundation), 03.12.2023

A case study summary, presenting periods corresponding to dominant peaks of Fourier spectra and transfer functions, is given in Table 9.

As it can be noticed from the first row of the table, the natural periods of vibration of the monitored building, without considering SSI (~0.16 - 0.18 s) are characteristic to a rigid structure, which is the case, considering its constructive system. The 0.18 s value results from the analysis of both earthquakes. It is interesting to notice that the 0.16 - 0.18 s value also represents the dominant peak of the transfer function for the vertical components of both earthquakes, which could indicate coupling between the horizontal and the vertical motion, possibly due to rocking or torsion, given the shape of the central section of the building, where sensors are located.

Table 9. Case study summary – BTH station, earthquakes on 31 January 2020 and on 3 December 2023 (in parentheses). Periods corresponding to the highest peaks of spectral and transfer functions

	Source	HNN channel	HNE channel	HNZ channel	Analysis outcome
1.	Transfer functions between the basement and the roof (04/B1)	0.167 s (0.179 s)	0.180 s (0.179 s)	0.157 s (0.180 s)	Natural periods of the structure, assuming a fixed base (no SSI)
2.	Fourier amplitude spectra & power spectra of the roof record (04)	0.235 s (0.314s)	0.306 s (0.288 s)	0.183 s (0.113 s)	Natural periods of the structure, considering soil–structure interaction (SSI)
3.	Fourier amplitude spectra & power spectra of the free field record (FF)	0.442 s (0.225 s)	0.330 s (0.181s)	0.235 s (0.254s)	Information on ground motion spectral content
4.	Fourier amplitude spectra & power spectra of the basement record (B1)	0.439 s (0.314 s)	0.328 s (0.311 s)	0.352 s (0.113 s)	Information on the frequency content of the motion at the building's foundation
5.	Transfer functions between the ground motion and the foundation motion (B1/FF)	0.256 s (0.272 s)	0.314 s (0.309 s)	0.256 s (0.256 s)	Kinematic effects at the buildings' foundation

Nevertheless, transfer function amplitudes are small in the amplification range. Most probably, 0.18 s is not the actual natural period of the building on the vertical direction, and possibly the 0.113 s value resulting from the analysis of the second earthquake could be a more plausible value.

The influence of the soil-structure interaction, reflected in the increase of the natural periods, can be noticed by comparing the values listed in the first two rows of the table. The exception occurs for the vertical component of the roof record on 03.12.2026, as explained above.

By analysing rows 3 and 4 of the table, it results that, for the horizontal components of the first earthquake, there is practically no influence of the presence of the building on the spectral content of the ground motion, in the case of the first earthquake. For the horizontal components of the second earthquake and for both vertical components, the highest peak values lack relevance due to the presence of multiple comparable peaks on the spectrum, which makes it difficult to discern the dominant periods.

Row 5 of the table illustrates the kinematic effects at the buildings' foundation. The dominant peaks of the transfer function are highly stable and show little variation across the two earthquakes, which suggests that the soil-foundation system moderately amplifies the ground motion over a rather narrow frequency band, i.e., 0.26 - 0.31 s, with higher values generally occurring only up to about 0.4 s.

It is important to note that the values in Table 9 should be interpreted only in correlation with the actual shape of the diagrams which they refer to. For instance, for many of the analysed graphs, multiple secondary peaks can be observed. Although their amplitudes are smaller than that of the dominant peak, they still indicate additional significant motion frequencies.

CONCLUSIONS

The article presented a detailed analysis of the seismic response of a higher education building that has been instrumented for over a decade and is located on the campus of the University

of Agronomic Sciences and Veterinary Medicine in Bucharest. Unlike many instrumented buildings in densely populated urban areas, the specific location of the building has allowed the installation of vibration sensors not only on the structure itself, but also within a nearby green space, thus enabling the continuous acquisition of co-located structural and free-field seismic records. The data recorded during two recent seismic events (local magnitude 5.2 and 4.8) originating in the seismogenic Vrancea zone of Romania were processed. Response spectra, Fourier amplitude spectra, power spectra, pseudovelocity spectra, normalized input energy spectra and transfer functions were computed, for free field, basement and roof records.

The most significant observations and conclusions are presented below.

- The natural periods of the building have been identified as ~0.17 s (HNN), ~0.18 s (HNE) – without considering soil-structure interaction (SSI), and ~0.24 s (HNN), ~0.31 s (HNE) – with the consideration of SSI. The vertical periods, more difficult to determine due to the broad frequency content of the motion are probably around 0.11 s. The values are in line with previous studies of the authors, based on a different approach (Dobre et al., 2024).
- The frequency content of the two considered earthquakes differs significantly, which also impacts the response of the soil-foundation system.
- The influence of the soil-structure interaction is considerable for the horizontal components of both earthquakes. Coupling between the horizontal and the vertical motion was also identified, indicating possible rocking or torsion effects.
- Kinematic effects at the foundation of the building are moderate and stable, being confined to a rather narrow frequency range.
- Complex resonance phenomena were identified with respect to different frequencies of the site, such that additional investigations are needed, especially concerning soil conditions determined from deeper borehole measurements.
- Pseudovelocity and normalized energy spectra provide important information on the spectral content of the ground motion and serve as indicators of the periods associated with the maximum destructive potential of the seismic motion. According to the results obtained, the most destructive period interval for both earthquakes considered in the study is situated between 0.2 and 0.6 seconds.

The results of the study gain additional relevance when considered in the dual context of the recent seismicity in Bucharest and of the need for the identification of the optimal approaches to the structural health monitoring of buildings located in densely populated urban areas.

ACKNOWLEDGEMENTS

This work was performed in the PNCDI 2022-2027 framework, within the “Nucleu” Programme PN 23 35 “ECODIGICONS”, Project PN 23 35 01 01 “Integrative concept for the digital analysis of data from the large-scale seismic monitoring of the national territory and of the building stock, intended for the rapid identification of the destructive potential of seismic events produced in Romania and in the adjacent regions”, with the support of the National Authority for Research. The maintenance and operation of the infrastructures used were supported by funding provided by UEFISCDI to the National Network for the Seismic Monitoring and Protection of the Building Stock (RNMPSPC–I.O.S.I.N.) at INCD URBAN-INCERC, through PNCDI IV, Programme 5.5 "Research Infrastructures". This financial support is gratefully acknowledged.

REFERENCES

Bălan, S., Cristescu, V. and Cornea, I. (coordinators) (1982). *The Romania Earthquake of 4 March 1977* (in Romanian). Bucharest: Editura Academiei.

Berg, G. V., Bolt, B. A., Sozen, M. A., & Rojahn, C. (1980). Earthquake in Romania March 4, 1977: An engineering report (Report No. PB82-163114). National Science Foundation. https://nehrpsearch.nist.gov/article/PB82-163114/XAB.

COSMOS (2001). *Guidelines for Installation of Advanced National Seismic System (ANSS) Strong-Motion Reference Stations*. Consortium of Organizations for Strong-Motion Observation Systems. Available online at https://www.strongmotion.org/ resources-publications/blog-post-title-four-c43d8-7pjna-8hmwj-cfg9y-xsceh-z5scn-cpx87

Dobre, D., Dragomir, C.S., Dobrescu, C.F., Craifaleanu, I.G., Georgescu, E.S., & Zaharia, M.C. (2024). The evolution of the dynamic characteristics of the soil-structure system in case of a university building seismic monitoring. *Scientific Papers. Series E. Land Reclamation, Earth Observation & Surveying, Environmental Engineering*, Vol. XIII, Print ISSN 2285-6064, 408-416.

Kashima, T. (2016). *ViewWave Manual*, January 2016, for Version 2.2.0. Available online at https://smo.kenken.go.jp/~kashima/ sites/default/files/viewwave/vwmanual220.pdf.

Kashima, T. (2024). *ViewWave* (Version 2.2.8) [Computer software]. Kashima's Office - BRI Strong Motion Network. https:// smo.kenken.go.jp/~kashima/view wave

Skolnik, D. (2010). *Free-field stations installation guidelines for post-event assessment of nearby structures*. Kinemetrics, U.S.A.